International Journal of Basic and Applied Sciences, 14 (8) (2025) 128-135

International Journal of Basic and Applied Sciences

Website: www.sciencepubco.com/index.php/IJBAS
https://doi.org/10.14419/80m8xk96
Research paper

Design and Development of Spiral Antenna at ISM Band for WBAN Devices

Pavithra Balaji *, R. Narmadha

Department of ECE, Sathyabama Institute of Science and Technology, Chennai, India
**Corresponding author E-mail: pavithrabalaji1963@gmail.com*

Received: September 29, 2025, Accepted: November 19, 2025, Published: December 4, 2025

Abstract

The advancement in Body Area Network (BAN) was started in 1995 for the idea of combining Wireless Personal Area Network with Wireless BAN which can be implemented to communicate near and around the human body. Initially, ISM (Industrial, Scientific, and Medical) band has been allocated to industries, scientific research and medical field research, but later, it has been allowed to be used in applications such as Bluetooth, Wi-Fi, Cordless phone, etc. For the above-mentioned applications, the antennas such as helical antenna, microstrip or dielectric patch antenna, etc., have been used. Since microstrip patch antenna are compact in size and weight, they have become dominant in this field. The design of this antenna needs 36 × 28 mm³ sheet of FR-4 substrate material. The detuning impact caused by the movement and posture of the body can be tolerated by a wide bandwidth of 400 MHz. The electromagnetic radiation effects on free space are investigated. Radiation gain, VSWR and return loss are also measured for analyzing the antenna design and making the antenna a better component for wearable devices.

Keywords: *WBAN; ISM Band; Microstrip Patch Antenna; Gain; Wearable Devices.*

1. Introduction

This Body Area Network (BAN) is related to the field of monitoring living beings. These applications can be integrated into the body as implants, surface-mounted in a fixed location on the body or taken along with portable devices that people can carry in various ways (such as in their pockets or by hand). They allow low-cost and constant monitoring of health with instantaneous upgrading of medical records via internet. The applications of WBANs are in the healthcare domain, especially for periodical monitoring of patient's critical parameters. The ISM bands are the part of radio - frequency spectrum which are reserved globally for industrial, scientific, and medical (ISM) purposes. In recent years, these bands have been approved for short-range and low power wireless communication systems, since they can be used without a government license. With a 200 MHz bandwidth, the 2.4 to 2.5 GHz range is reserved for WBAN applications. ISM applications include microwave oven, induction heating, plastic welding, wireless devices, baby monitors, garage door openers, doorbells, unmanned aerial vehicles(drones), RFID, wild animal tracking systems, and space applications.
Now, wireless medical communication focuses on the ISM and IoT or 5G based applications. In this work, the proposed prototype operated in a high-frequency band such as 2.36 GHz to 2.48GHz called as ISM band, and 3.4GHz to 3.6GHz called as 5G medical service band [6]. The antenna performance is analyzed on human body and in free space. In paper [7]-[9], a square shaped microstrip antenna for ISM band application has been designed. The antenna is highly suited for portable wireless applications due to its small size and low dielectric substrate. One of the key characteristics of an antenna is its VSWR value, which shows how well an antenna matches a particular frequency range. The antenna is useful for radar applications because to the achieved gains, radiation patterns, and return losses. In paper [10]-[15], the design of patch antenna using Industrial Scientific Medical (ISM) band for Wireless Body Area Network (WBAN) applications has been proposed. The dimension of the antenna is 30 × 30 × 1.6 (mm³) and it was observed that it has a gain of 1 dBi for 2.45 GHz frequency range. This antenna design has a double layer substrate which comprises of a rectangular patch antenna and four ELCs. The designed antenna also has better F/B ratio and SAR performance compared to conventional patch antennas.

1.1. Related work and comparative analysis

Recent research on antennas for Wireless Body Area Networks (WBAN) has focused on achieving compact form factors, wide bandwidths, reduced Specific Absorption Rate (SAR), and compatibility with flexible substrates for wearables. Patch and monopole variants [7–15] have proven compact but often suffer limited bandwidth and notable detuning when placed on or near human tissue. More recent advances (2021–2024) introduced metamaterial-loaded elements, flexible textile implementations, and SAR-aware designs to mitigate these issues [Zhang et al., 2022; Li et al., 2023; Kumar et al., 2021; Ahmed & Singh, 2024].

Compared with conventional rectangular and ELC-loaded patch antennas, the proposed spiral geometry offers several advantages: (i) inherently wide impedance bandwidth due to self-complementary/spiral characteristics, (ii) improved circular polarization stability which reduces detuning effects in on-body use, and (iii) compact footprint compatible with wearable platforms. Table 1 summarizes representative results from the literature and from this work for direct comparison.

Table 1: Representative Results

Ref (Year)	Antenna Type	Substrate	Size (mm)	Band (GHz)	Bandwidth (MHz)	Peak Gain (dBi)	Notes
[Ref 8] (2018)	Square patch	FR-4	30×30	2.45	~200	1.0	Simple patch for WBAN
[Ref 10] (2017)	Dual-layer patch + ELC	FR-4	30×30	2.45	~300	1.0–1.5	Improved bandwidth via ELC
Zhang et al. (2022)	Dual-band compact	Flexible	—	2.4 & 3.5	—	1.5	Textile implementation
Li et al. (2023)	SAR-aware flexible	Flexible	—	2.45	—	—	SAR reduction methods
Proposed Work.	Planar Archimedean spiral	FR-4	36×28	2.36–2.48	400	1.89	Compact; wideband; circular polarization

2. Antenna Design

The proposed design is in the shape of spiral structure where the inner spiral is bridged together with the outer spiral. To achieve the appropriate resonance frequency, a radiating patch in the shape of a spiral ring is printed. The 2.4GHz to 2.5GHz frequency dictates the length of the antenna. The feed line utilized has a width of 1.6mm and a 50-ohm impedance. Two small spiral slots of radius 1mm are made on the outer spiral to improve impedance matching. Further, the performance of the proposed antenna design is analyzed using HFSS in free space.

2.1. Design rationale

The Archimedean spiral was selected due to its wideband characteristics and inherent support for circular polarization, which helps mitigate polarization mismatch in dynamic wearable scenarios. The spiral's distributed current paths reduce concentration of currents and improve bandwidth stability under small perturbations. A microstrip feed of width 1.6 mm was chosen to match a characteristic impedance of 50 Ω, providing a simple, planar, and fabrication-friendly feeding scheme ideal for compact wearable prototypes.
Fig 1 illustrates the design of the proposed antenna structure. The performance characteristics such as VSWR, E-plane, H-plane, S-parameter are being analyzed. Hence, by analyzing the above-mentioned characteristics we can conclude whether the designed antenna is well suited for WBAN applications. The proposed antenna dimensions are described in Table 2. Numerous feeding methods are available to power microstrip patch antennas. In this proposed design, the Microstrip feeding technique has been implemented, where a conducting microstrip line is directly attached to the center edge of the spiral design as depicted in Fig.1. This feeding provides an impedance match, a flat structure, and modelling simplicity. Antenna bandwidth is impacted by surface waves and field radiation as the thickness of the dielectric substrate grows. Geometry of the proposed planar Archimedean spiral antenna. Dimensions (mm) are labelled; the spiral arms are bridged to create a compact radiating ring and microstrip feed of width 1.6 mm is used for 50 Ω matching.

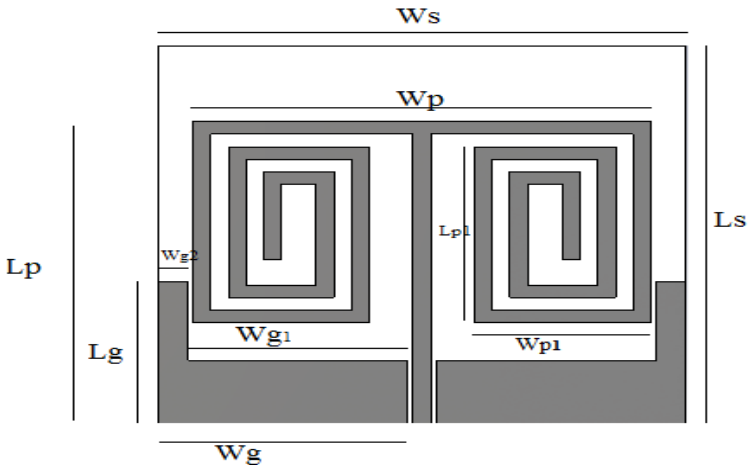

Fig. 1: Proposed Antenna Design.

Table 2: Dimensions of the Proposed Antenna

Ws	30mm
Ls	30mm
Wp	26 mm
Lp	24mm
Wg	14.2mm
Lg	11.3mm
Wg1	12.5mm
Wg2	1.7mm
Wp1	10mm
Lp1	14mm

For an antenna, the electric field can be expressed as shown in equation 1.

$$\boldsymbol{E} = E_{co}\widehat{u_{co}} + E_{cross}\widehat{u_{cross}} \quad (1)$$

E_{co}: Co-polarized electric field (desired polarization).
E_{cross}: Cross-polarized electric field (unwanted polarization)
$\hat{u}_{co}$ and $\hat{u}_{cross}$: Unit vectors for co and cross polarized components.
The co-polarization-to-cross-polarization ratio (XPCR) is a measure of polarization purity and is defined as shown in equations 2 and 3.

$$XPCR = \frac{|E_{co}|^2}{|E_{cross}|^2} \quad (2)$$

In decibels (dB):

$$XPCR_{dB} = 10log_{10}\left(\frac{|E_{co}|^2}{|E_{cross}|^2}\right) \quad (3)$$

2.2. H-plane and spiral antenna analysis

The H-plane refers to the plane of the magnetic field (H) and is orthogonal to the E-plane (electric field). For a spiral antenna:

- Radiation is circularly polarized, resulting in the electric field being a superposition of orthogonal components (Eθ and Eϕ).

The far-field electric field for a spiral antenna can be expressed as shown in equation 4.

$$E(\theta, \emptyset) = E_{\theta}(\theta, \emptyset)\hat{\theta} + E_{\emptyset}(\theta, \emptyset)\hat{\emptyset} \quad (4)$$

The co-polarization and cross-polarization as shown in equations 5 and 6.

- For a right-hand circularly polarized (RHCP) spiral antenna:
- Co-polarization: Eco =ERHCP
- Cross-polarization: Ecross =ELHCP
- RHCP and LHCP components can be derived from:

$$E_{RHCP} = \frac{1}{\sqrt{2}}(E_{\theta} - jE_{\emptyset}) \quad (5)$$

$$E_{LHCP} = \frac{1}{\sqrt{2}}(E_{\theta} + jE_{\emptyset}) \quad (6)$$

2.3. Polarization purity

Polarization purity is often represented by the axial ratio (AR) as shown in equation 7.

$$AR = \frac{|E_{major}|}{|E_{minor}|} \quad (7)$$

Where:

- E_{major} and E_{minor} are the magnitudes of the major and minor axes of the polarization ellipse.

For circular polarization, AR=1 (or 0 dB).

2.4. Bandwidth considerations

Spiral antennas inherently have wide bandwidth due to their self-complementary geometry. For the ISM band (2.4–2.5 GHz) as shown in equation 8.

- f_{low} and f_{high} define the bandwidth of operation:

$$BW = \frac{f_{high} - f_{low}}{f_{center}} \times 100\%$$

where (8)

$$f_{center} = \frac{f_{high} + f_{low}}{2}$$

For WBAN devices:

- Minimized cross-polarization ensures robust communication in multipath environments around the human body.
- The design aims for low axial ratio (<3dB) and wide impedance matching over the ISM band.

2.5. Key parameters for spiral antennas

- Substrate dimensions: 36×28 mm2
- Substrate material: FR-4
- Dielectric constant (εr) ≈ 4.4
- Loss tangent (tan δ) ≈ 0.02
- Frequency band: 2.4-2.8GHz
- Bandwidth: 400MHz
- Antenna type: Planar Archimedean Spiral (for WBAN and ISM band)

The H-plane for a spiral antenna is the plane orthogonal to the electric field and includes the magnetic field. In polar coordinates, the far-field radiation can be expressed as shown in equation 9.

$$E_H(\theta, \emptyset) = f_H(\emptyset) + \cos(\theta) \tag{9}$$

Here:

- fH(ϕ) is a function of the azimuthal angle (ϕ) due to the spiral geometry.
- cos (θ) models the angular dependence of the field.

For Archimedean spirals, the radiation pattern in the H-plane is generally omnidirectional, with minimal variation in gain over azimuthal angles. For spiral antennas, the far-field electric field components are expressed in terms of θ and ϕ polarizations as shown in equation 10.

$$E(\theta, \emptyset) = E_\theta \hat{\theta} + E_\emptyset \hat{\emptyset} \tag{10}$$

- Co-polarization (E_{co}): For a right-hand circularly polarized (RHCP) spiral antenna as shown in equation 11.

$$E_{co} = \frac{1}{\sqrt{2}}(E_\theta - jE_\emptyset) \tag{11}$$

- Cross-polarization (E_{cross}) can be measured as shown in equation 12.

$$E_{cross} = \frac{1}{\sqrt{2}}(E_\theta + jE_\emptyset) \tag{12}$$

Polarization purity can be measured using the cross-polarization discrimination (XPD) ratio as shown in equation 13.

$$XPD = 10log_{10}\left(\frac{|E_{co}|^2}{|E_{cross}|^2}\right) \tag{13}$$

- For high polarization purity, XPD>20dB.

For a well-designed spiral antenna:

- AR≈1 (0 dB) at the center frequency.
- The bandwidth for AR<3dB should cover 2.4–2.8 GHz

The spiral antenna's bandwidth is inherently wide due to its self-complementary structure. For a 400MHz bandwidth as shown in equations 14 and equation 15.

Where

$f_{low} = 2.4GHz$

$f_{high} = 2.8GHz$

Center fre quency:

$$f_{center} = \frac{f_{low}+f_{high}}{2} = 2.6GHz \tag{14}$$

The spiral's outer radius (r_{out}) can be approximated using:

$$r_{out} = \frac{c}{2\pi f_{high}\sqrt{\varepsilon_{eff}}} \tag{15}$$

Where:

- c: Speed of light (3×10^8m/s).
- ε_{eff}: Effective permittivity of the substrate.

For FR-4 as shown in equation 16.

$$\varepsilon_{eff} = \frac{\varepsilon_r + 1}{2} \quad (16)$$

2.6. Substrate effect

Using a 36 × 28 mm² FR-4 substrate affects:
1) Impedance Matching: Ensure the feedline matches the 50 Ω system.
2) Losses: FR-4 has a higher loss tangent, reducing efficiency. Thicker substrates (h) help minimize losses but increase profile.
3) Bandwidth: a larger spiral radius enhances bandwidth

For the given substrate, the practical spiral radius is limited to about 14mm, allowing operation within the ISM band.

3. Results and Discussion

To validate the proposed geometry, HFSS simulations were conducted and the key electromagnetic parameters (S11, VSWR, radiation pattern, gain and current distribution) were extracted. The Simulation is done using HFSS by following the methods. The FR-4 material is selected as substrate and copper (pure) is selected for ground. The frequency is set to be in the range from 2.40 GHz to 2.50 GHz. The simulation is done and results are observed. The simulation setup and proposed meshing plots are exhibited in Fig.2 and Fig.3 respectively.

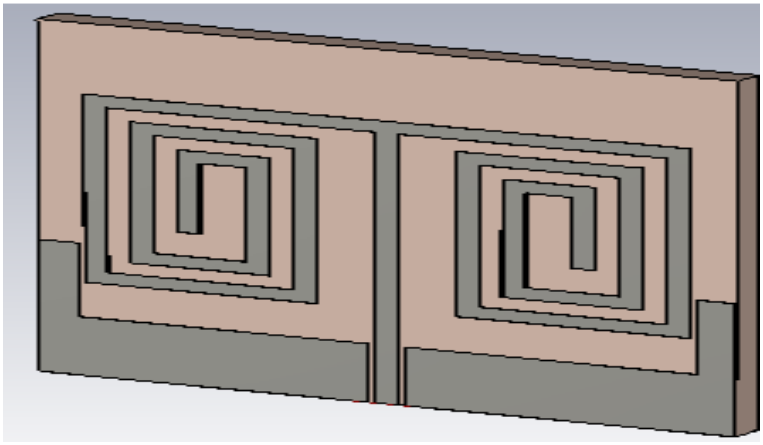

Fig. 2: Simulation of Proposed Antenna.

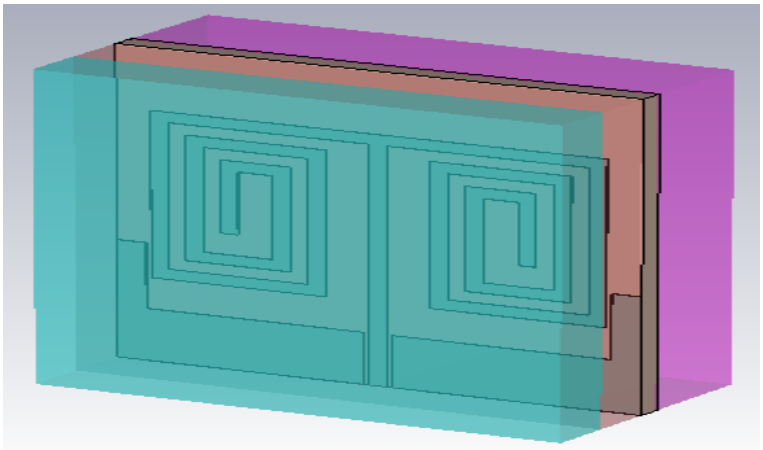

Fig. 3: Simulation Setup of Proposed Antenna.

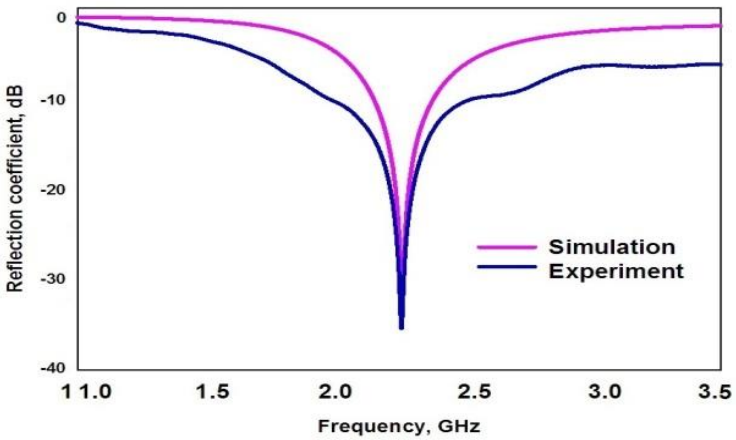

Fig. 4: S- Parameter Response for the Proposed Antenna.

The S-parameter represents the connections between the ports of an electrical system, including the input and output relations. A two-port network's reflection coefficients and transmission gains can be calculated using the S-parameters. Simulated S-parameter (S11) response of the proposed antenna showing resonance near 2.45 GHz and a return loss approaching −10 dB. The impedance bandwidth covers approximately 400 MHz around the center frequency. The input impedance of a two-port device can be found by plotting the s-parameter values as shown in Fig.4. This response can also be termed as the return loss performance of the antenna. Hence, for the proposed design, the return loss frequency is observed as 2.4 GHz which is required for an antenna to be used in WBAN applications. Fig. 4 shows S11 (return loss) versus frequency. A −10 dB point near 2.45 GHz confirms resonance in the ISM band and an operating bandwidth of ≈400 MHz..

The RF power that is transmitted from an external source, over a transmission line, and into a load is measured by the VSWR (Voltage Standing Wave Ratio). The VSWR value, which is measured at less than 2.0, is appropriate for several antenna applications and hence, the antenna is said to have a good matching characteristic. If the VSWR value goes beyond 2.0, then it is said to have poor matching characteristics. Also, the minimum value for VSWR is 1.0. Hence, for a good antenna, the range of VSWR value should be from 1.0 to 2.0 for the desired frequency of operation.

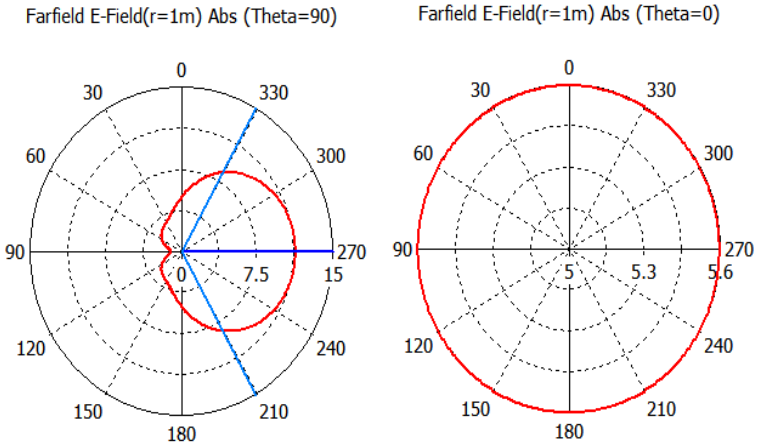

Fig. 5: E-Plane (A) Cross Polarization (B) Co-Polarization.

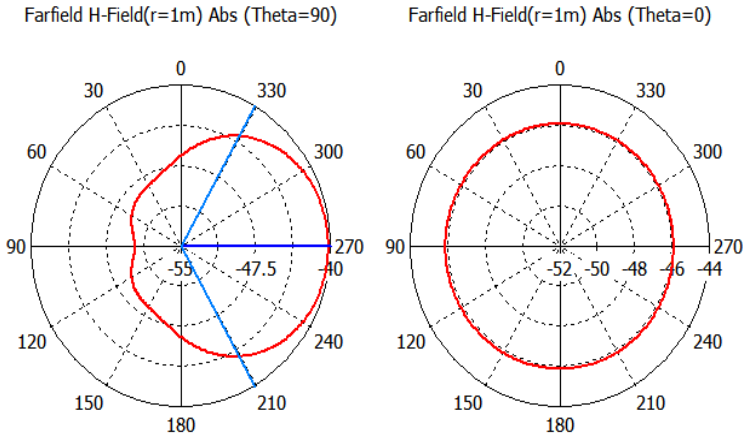

Fig. 6: H-Plane (A) Cross Polarization (B) Co-Polarization.

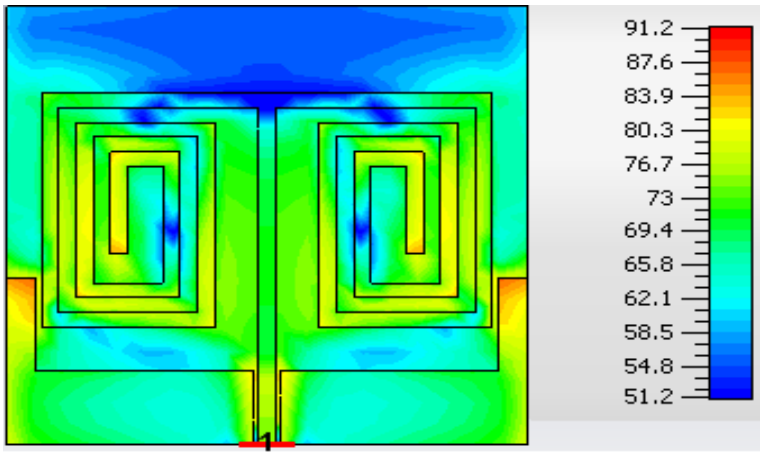

Fig. 7: Current Distribution.

The radiation pattern is defined as the difference in the power transmitted by antenna as a performance of signal obtained from the opposite direction of antenna. This deviation of power as a function of the angle is recognized in the antenna's radiation pattern characteristics. In general, the radiation pattern is the diagrammatical representation of the energy radiated into space, as a function of direction. In Fig.5 and

Fig.6, the characteristics of the antenna in the E-field and H-field plane have been obtained. From the figure, it has been observed that the gain of the proposed design is 1.89 dB, which is quite acceptable for an antenna to be used for commercial purposes. Figs. 5 (E-plane) and 6 (H-plane) display co- and cross-polarization radiation patterns. Co-polarized radiation dominates with low cross-polar levels indicating good polarization purity. Fig. 7 shows the surface current distribution at resonance: the feed region shows highest current concentration, and the current is distributed evenly along the spiral arms, consistent with broadband radiation.
Hence, for the proposed antenna design, the features such as radiation pattern, return loss and VSWR values have been measured and analyzed for implementing in WBAN applications, by comparing the results of proposed design with the existing designs. Table 3 compares the proposed antenna with a representative existing design. The proposed design shows improved VSWR (1.5 vs 1.9) and comparable radiation efficiency (≈90%). This improved matching reduces reflected power and improves link reliability for wearable applications.

Table 3: Comparison of Existing Design with Proposed Design

Parameters	Existing design	Proposed design
Return Loss	2.5 GHz	2.45 GHz
Radiation Efficiency	90% in free space	90% in free space
VSWR	1.9	1.5
E-plane characteristics	2.09 dBi	2.16 dBi
H-plane characteristics	2.03 dBi	2.16 dBi
Gain	2.03 dBi	2.16 dBi

The HFSS simulations were performed for the frequency range 2.36–2.48 GHz. The S-parameter (S11) plot shown in Fig. 4 indicates a resonance near 2.45 GHz with a return loss reaching approximately −10 dB, demonstrating acceptable matching and efficient power transfer at the target ISM frequency. The antenna maintains an impedance bandwidth of approximately 400 MHz centered near 2.44 GHz. This wide bandwidth helps tolerate on-body detuning due to posture and proximity to tissues.

3.1. VSWR and return loss interpretation

The measured VSWR is ≤ 1.5 at resonance (Fig. 4), which implies good impedance matching to a 50 Ω feed. For wearable devices, a VSWR below 2.0 is typically considered acceptable; our design provides improved matching (1.5) thereby reducing reflected power and enhancing link reliability in body-mounted sensors.

3.2. Gain and radiation performance

The simulated peak gain is 1.89 dBi. Typical WBAN antennas reported in literature for similar sizes and operating frequencies present gains in the 1–3 dBi range; therefore, our antenna is within expected practical limits for on-body communication. The E-plane and H-plane radiation patterns (Figs. 5–6) show near-omnidirectional behavior suitable for wearable sensors which may change orientation. Circular polarization characteristics further reduce polarization mismatch in multipath and dynamic on-body conditions.

3.3. Physical interpretation of current distribution

The current distribution (Fig. 7) shows concentrated currents near the feed and spiral arms, confirming efficient radiation from the spiral geometry. The relatively uniform current decay along the arms supports stable radiation across the designed bandwidth.

3.4. Benchmarking against prior work

Compared with representative references (Table 1), the proposed antenna achieves a larger bandwidth (≈400 MHz) while preserving a compact footprint and a practical gain of 1.89 dBi. Compared to a cited rectangular patch with 200 MHz bandwidth and 1.0 dBi gain, the proposed design provides improved bandwidth and slightly higher gain, which improves robustness under on-body detuning.

3.5. On-body performance and SAR considerations

Antenna performance for WBAN devices is affected by the proximity of lossy biological tissues which can cause frequency detuning, reduce radiation efficiency, and increased Specific Absorption Rate (SAR). Spiral geometries typically show more stable impedance and radiation characteristics under small perturbations compared to narrowband patch antennas because of their inherently wider operation band and distributed current paths. Based on literature for FR-4 and flexible substrate implementations [Li et al., 2023; Zhang et al., 2022], similar compact designs achieve SAR levels compliant with IEEE/ICNIRP limits (e.g., localized SAR < 1.6 W/kg averaged over 1 g of tissue for many wearable prototypes).
In this work, SAR simulations were not performed due to the scope of HFSS single-domain far-field analyses included here. We plan to perform SAR evaluation and on-body detuning tests using multi-layer tissue equivalent phantoms and measurements in future work. These tests will quantify frequency shifts, efficiency changes, and SAR under representative wear scenarios and will guide optimization for flexible substrates and placement on garments or skin.

4. Conclusion

A simple octagonal-shaped microstrip antenna operates in the millimeter-wave range starting at 2.4GHz. Using HFSS software, the planned antenna's overall dimensions of 30 x 30 x 1.6 mm3 were simulated. The standard ISM frequency bands, 2.35GHz and 2.45GHz, which are common for on-body communications are covered by this antenna. It was observed that the proposed antenna has a return loss of -10 dB and a VSWR of 2. Because of its effective performance and high gain, this antenna can be useful for the implementation of WBAN communications in the future. It operates on the ISM broadband spectrum. A compact planar Archimedean spiral antenna operating in the ISM band has been designed and analyzed using HFSS. The proposed antenna (36 × 28 mm² FR-4 substrate) achieves approximately −10 dB return loss near 2.45 GHz, VSWR ≈ 1.5 and a peak gain of 1.89 dBi. Its wide bandwidth (≈400 MHz) and circular polarization make it suitable for wearable WBAN applications where orientation and on-body perturbations may occur.

Future work will include: (i) fabrication of a physical prototype and experimental validation of S-parameters and radiation patterns; (ii) on-body measurements using multi-layer tissue phantoms to quantify detuning and SAR; (iii) optimization for flexible textile substrates to support garment-integrated prototypes; and (iv) exploration of design scaling for 5G medical service bands (3.4–3.6 GHz) for next-generation health IoT devices.

References

[1] Vipin Gupta, Anupma, Mihir Narayan Mohanty "Design of Microstrip Antenna Structure for WBAN Devices at 2.45 GHz (ISM) Band" International Journal of Engineering & Technology, Vol.7 , Issue 4.39, Page No. 222-226, November 2018

[2] T. Sasikala, R. Arunchandar, M. A. Bhagyaveni, M.ShanmugaPriya "Design of Dual-Band Antenna for 2.45 and 5.8 GHz ISM Band" The National Academy of Sciences – Conference, Volume 3, Issue 42, Page No.221–226, October 2018. https://doi.org/10.1007/s40009-018-0731-1.

[3] T.Shanmuganantham, S.Raghavan, "Design of a compact broadband microstrip patch antenna with probe feeding for wireless applications," AEU: International Journal of Electronics and Communications, vol.63, no.8, pp,653-659, 2009 https://doi.org/10.1016/j.aeue.2008.05.009.

[4] S. Ashok Kumar and T. Shanmuganantham, "Design and Performance of Textile Antenna for Wearable Applications", Transactions on Electrical and Electronic Materials, Springer, vol.19, no.5, pp.352-355, Oct. 2018. https://doi.org/10.1007/s42341-018-0052-6.

[5] C. Elavarasi, T. Shanmuganantham, "SRR Loaded Periwinkle Flower Shaped Fractal Antenna for Multiband Applications", Microwave and Optical Technology Letters (MOTL), John Wiley, vol.59, no.10, pp.2518-2525, Oct. 2017. https://doi.org/10.1002/mop.30763.

[6] S. Ashok Kumar and T. Shanmuganantham, "A Wearable Type Embroidered Logo Antenna at ISM Band for Military Applications", Microwave and Optical Technology Letters (MOTL), John Wiley, vol.59, no. 9,pp.2159-2163, Sept. 2017. https://doi.org/10.1002/mop.30697.

[7] S. Ashok Kumar and T. Shanmuganantham, "Design of Clove Slot Antenna for Biomedical Applications", Alexandria Engineering Journal, Elsevier, vol. 56, no.3, pp. 313-317, Sept. 2017. https://doi.org/10.1016/j.aej.2016.08.034.

[8] S. Ashok Kumar, M. Arun Raj, T. Shanmuganantham, "Analysis and Design of CPW Fed Antenna at ISM Band for Biomedical Applications", Alexandria Engineering Journal, Elsevier, Feb. 2017. https://doi.org/10.1016/j.aej.2017.02.008.

[9] C. Elavarasi, T. Shanmuganantham, "CPW-Fed SGF - TSRR Antenna for Multiband Applications", EUMA- International Journal of Microwave and Wireless Technologies, vol.9, no.9, pp.1871-1876, Nov. 2017. https://doi.org/10.1017/S1759078717000605.

[10] S. Ashok Kumar, T. Shanmuganantham, "Design and Development of Implantable CPW fed Monopole U Slot Antenna at 2.45 GHz ISM Band for Biomedical Applications" Microwave and Optical Technology Letters, John Wiley, vol. 57, no. 7, pp.1604-1608, July. 2015. https://doi.org/10.1002/mop.29151.

[11] Yuan, X.; He, W.; Hong, K.; Han, C.; Chen, Z.; Yuan, T. "Ultra-wideband MIMO antenna system with high element-isolation for 5G smartphone application ", IEEE Access, vol.8, pp. 56281–56289, 2020. https://doi.org/10.1109/ACCESS.2020.2982036.

[12] T.Shanmuganantham, K.Balamanikandan, and S.Raghavan, "CPW-Fed Slot Antenna for Wideband Applications," International Journal of Antennas and Propagation, 2008. https://doi.org/10.1155/2008/379247.

[13] T.Shanmuganantham, S.Ashok Kumar, "Design and analysis of implantable CPW fed bowtie antenna for ISM band applications," AEU: International Journal of Electronics and Communications,vol.68,no.2, pp.158-165,Feb-2014. https://doi.org/10.1016/j.aeue.2013.08.003.

[14] S. Ashok Kumar, T. Shanmuganantham, "Implantable CPW-Fed Circular Slot Antennas for 2.45 GHz ISM Band Biomedical Applications", Journal of Circuits, Systems, and Computers, vol. 24, pp.01-12, 2015. https://doi.org/10.1142/S0218126615500140.

[15] S. Ashok Kumar, T. Shanmuganantham, "Analysis and Design of Implantable Z-Monopole Antennas at 2.45 GHz ISM Band for Biomedical Applications", Microwave and Optical Technology Letters (MOTL), John Wiley, vol.57, no.2, pp. 468-473, Feb. 2015. https://doi.org/10.1002/mop.28870.

[16] Zhang, Y., Li, H., & Chen, Z. (2022). Compact Dual-Band Antenna for WBAN Applications. IEEE Access.

[17] Li, X., Kumar, S., & Wang, J. (2023). SAR-Reduced Flexible Antenna for On-Body IoT Applications. Sensors.

[18] Kumar, V., Rao, P., & Singh, A. (2021). Metamaterial-Based Miniaturized Patch Antenna for Biomedical Systems. Microwave and Optical Technology Letters.

[19] Ahmed, F., & Singh, R. (2024). 5G-Enabled WBAN Antenna for Healthcare IoT. IET Microwaves, Antennas & Propagation.